JOC The Journal of Organic Chemistry
Article
Cite This: J. Org. Chem. 2020, 85, 85−91
pubs.acs.org/joc

Amplification of the Quantum Yields of 2-λ^5-Phosphaquinolin-2-ones through Phosphorus Center Modification

Jeremy P. Bard,[†] Hannah J. Bates,[†] Chun-Lin Deng,[†] Lev N. Zakharov,[‡] Darren W. Johnson,[*,†] and Michael M. Haley[*,†]

[†]Department of Chemistry & Biochemistry and the Materials Science Institute, University of Oregon, Eugene, Oregon 97403-1253, United States

[‡]CAMCOR, University of Oregon, Eugene, Oregon 97403-1433, United States

Supporting Information

ABSTRACT: We report the synthesis and characterization of P-phenyl modified phosphorus- and nitrogen-containing phosphaquinolinone heterocycles. The change from −OPh to −Ph results in a marked increase in the quantum yield of the scaffold as well as a moderate red-shifting of the emission. While calculations suggest that π to π^* transitions are dominant, intramolecular charge transfer (ICT) also contributes in the excited state. Solution- and solid-state studies of the dimerization of this new congener to the P-phenoxy variant are also reported, showing retention of the dimerization behavior in this scaffold.

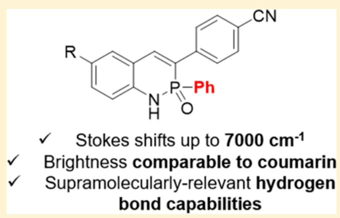

■ INTRODUCTION

Small molecule fluorophores are used ubiquitously throughout many different fields, including chemical biology, molecular probe development, and materials for industrial and environmental sensing.[1−4] In many of these applications, a fluorophore must exhibit a few characteristics to be considered optimal: large Stokes shift, high brightness, and red-shifted emission. One such example of a molecule that meets these specifications is coumarin (Figure 1).[5−14] An impressive number of

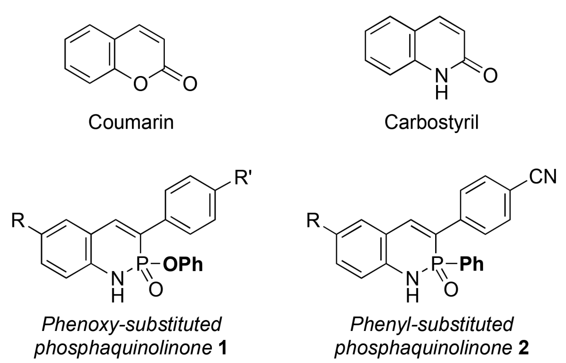

Figure 1. Well-studied coumarin and carbostyril scaffolds (top) compared to phosphaquinolinone analogues (bottom).

coumarin-containing compounds have been reported throughout the literature that are collected either from in-lab syntheses or by isolation from natural sources.[15,16] This scaffold has been the subject of a variety of synthetic modifications, diversification by adding groups onto the backbone, or incorporation of the coumarin system into larger ring networks.[17−19] Through these modifications, a tremendous breadth of understanding upon the structure−activity relations has been developed[20−24] that have guided the design of many useful derivatives, which have emerged for applications in chemosensing and many other areas.[25−31]

Alongside the many derivatives of the parent coumarin scaffold, there is the nitrogen-containing structural analogue known as carbostyril (Figure 1).[32−37] Though not as widely utilized as coumarin, carbostyril is the subject of many structure−property relationship studies, and it shows promise for use in both pharmaceutical discovery and fluorescence imaging applications.[38,39] These carbostyril analogues expand on the applications of the coumarin family through modifying the lactone core to a lactam. With further alteration of this core, new applications, functionality, and fluorescent properties are expected from this widely used fluorophore.

Recently, we reported a series of phosphorus- and nitrogen-containing (PN) phosphaquinolinone **1** derivatives (Figure 1).[40,41] This scaffold, which is one of only a handful of similar heterocycles,[42−52] is also an isostere to carbostyril and coumarin, with the only difference being the replacement of the lactam carbonyl with an isolobal, chiral phosphorus center. We have performed a variety of structure−property studies that looked at the effects of both acene core modification and substitution at various points on the scaffold.[40,41,53−56] In these studies, it was found that the emission wavelength can be moderately red-shifted through careful substitution of various groups on the backbone, affording significant Stokes shifts and modest quantum yields. On the basis of these design principles, this moiety has recently been implemented in a fluorescent receptor for HSO_4^- in acidic media, showing promise for future applications of this scaffold that take advantage of both its exceptional hydrogen bonding

Special Issue: Functional Organic Materials

Received: August 2, 2019
Published: September 30, 2019

DOI: 10.1021/acs.joc.9b02132
J. Org. Chem. 2020, 85, 85−91

capabilities and its inherent fluorescence.[54] As clearly shown for the coumarin and carbostyril motifs, systematic modification of various structural aspects can lead to very useful derivatives. In our continuing efforts to study the 2-λ^5-phosphaquinolin-2-one skeleton, the next facet that we wanted to explore was the variation of the group attached to the phosphorus center. Disclosed herein is the substitution of a phenyl ring in place of the standard phenoxy upon the phosphorus center, generating a racemic mixture of heterocycle **2** (Figure 1). We also hypothesize that this would increase the quantum yield through rigidifying the scaffold. With these modifications, the reported compounds could have greater potential for applications in phosphorus-containing chemosensors and fluorophores, expanding on this pre-existing group of molecules.[57−65]

■ RESULTS AND DISCUSSION

The synthesis of **2** starts from key arylethynylaniline intermediate **3**, prepared following previously reported methods.[40] Aniline **3** is then reacted with diphenyl phenylphosphonite ($PhP(OPh)_2$) in pyridine at 100 °C. Subsequent hydrolysis in THF at 60 °C furnishes phenyl-appended

Scheme 1. Synthesis of Phosphaquinolinones 2

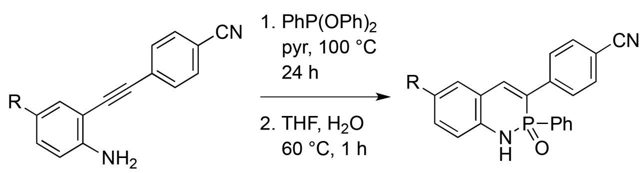

3

heterocycles **2** in modest to good yields (Scheme 1). ^{1}H, ^{13}C, ^{31}P, and ^{19}F NMR spectra were collected for **2** (see Supporting Information), which reveal that the direct attachment of the phenyl ring to the phosphorus center not only splits the signals of the phenyl ring ($J_{^{31}P,^{1}H}$ and $J_{^{31}P,^{13}C}$ values listed in the Experimental Section) but also affords coupling constants of *ca.* 30 Hz ($^3J_{^{31}P,^{1}H}$) for the alkene proton signal.

The photophysical properties of **2a**−**2f** in $CHCl_3$ are shown in Figure 2 and are compiled in Table 1. All derivatives share a common λ_{max} at *ca.* 300 nm, and the lowest energy absorption peaks range from 343 to 381 nm. The absorption coefficients for this scaffold stay within the range of 1.5×10^4 (for **2a**) to 2.2×10^4 M^{-1} cm^{-1} (for **2e** and **2f**). The λ_{em} values range from 447 (for **2a**) to 515 nm (for **2f**) with Stokes shifts on the order of 6350−7000 cm^{-1}. Interestingly, the emission spectra of **2** show a *ca.* 20 nm bathochromic shift from those of the analogous congeners of **1**,[40] and the quantum yields of this scaffold show a dramatic improvement, on the order of a 4−5-fold increase in most cases. Brightness values range from 6.84×10^3 (for **2b**) to 1.14×10^4 M^{-1} cm^{-1} (for **2a**), which are now on par with several optimized coumarin derivatives.[66]

Fluorescence lifetime measurements were also performed (Figure S6), and the radiative (k_r) and nonradiative (k_{nr}) decay rate constants were determined. The k_r values range from 0.06 to 0.19 ns^{-1}, and the k_{nr} values vary from 0.06 to 0.18 ns^{-1},

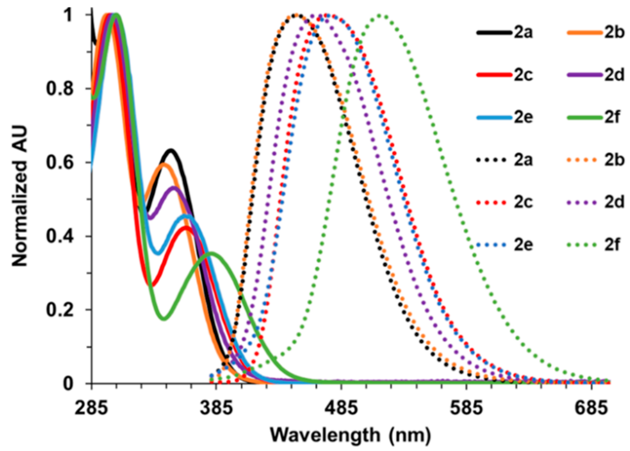

Figure 2. Absorption (solid lines) and fluorescence (dotted lines) spectra of **2** in $CHCl_3$ at 298 K.

showing either equal rates or a slightly larger k_{nr} in most cases. These values elucidate a potential explanation for the increased quantum yields when compared to similar values of phosphaquinolinones **1**.[40] For **1**, the k_r values range from 0.10 to 0.30 ns^{-1}, which show similar values, whereas the k_{nr} values vary from 0.30 to 3.0 ns^{-1}, which are substantially faster in most cases. The diminished ratio of k_{nr} to k_r seen for **2** may suggest that the reduced degrees of freedom may indeed be the cause of the increased quantum yields.

To gain further understanding of these experimental results, the frontier orbitals for heterocycles **2** were calculated (Tables 1 and S1−S7). The narrowest HOMO−LUMO gap is seen for **2f** (3.90 eV), and the largest is for **2a** (4.40 eV). This trend arises because of a higher magnitude of HOMO destabilization than that of the stabilization of the LUMO with more donating substituents (Table S1). These values also follow a similar trend to the optical gaps (Table 1). TD-DFT was then used to examine the S_0 to S_1 transition. It was found that the S_0 to S_1 transition is dominated by the HOMO−LUMO transition (Table S1). Additionally, the distributions of the HOMOs and LUMOs show a slightly more pronounced separation due to a larger HOMO localization at the phosphorus center (Figure S4). These observations suggest that π to π^* transitions are dominant, but there may be some intramolecular charge transfer (ICT) occurring in the excited state. The emission of **2** was then examined in solvents of varying polarities (Figures S7−S13 and Tables S11−S16). In these studies, bathochromatic shifting is observed in every case with more polar solvents. Compound **2f** showed the greatest shifting, ranging from emission wavelengths of 504 to 531 nm and Stokes shifts of 6070 and 7070 cm^{-1} in cyclohexane and acetonitrile, respectively.

The TD−DFT optimized S_1 state near the Franck−Condon geometry of **2f** shows that the dihedral angle between the parent core and appended 4-cyanophenyl substituent becomes smaller compared to the ground state (Figure 3). Additionally, the C−C bond connecting them is shortened by *ca.* 0.035 Å. The considerable geometric changes lead to a more conjugated system at the S_1 state, in which the HOMO−LUMO energy gap decreases by 0.9 eV (Figure S5); thus, the computed emission wavelength of 541 nm is within the observed emission maxima (Table 1). These computational results could further explain the large Stokes shift for this type of PN-heterocycle.

DOI: 10.1021/acs.joc.9b02132
J. Org. Chem. 2020, 85, 85−91

Table 1. Photophysical Properties and HOMO−LUMO Energy Gaps of Heterocycles 2[a]

cmpd	λ_{abs} (nm)/ε (M^{-1} cm^{-1})	λ_{em} (nm)/ϕ (%)	Stokes shift (cm^{-1})	τ[b] (ns)	k_r (ns^{-1})	k_{nr} (ns^{-1})	ΔE_{opt} (eV)	ΔE_{DFT} (eV)[c]
2a	348/15000	447/76	6360	4.1	0.19	0.06	3.19	4.40
2b	343/18000	449/38	6880	3.5	0.11	0.18	3.18	4.43
2c	360/19000	474/43	6680	4.8	0.09	0.12	3.05	4.23
2d	352/18000	467/50	7000	3.9	0.13	0.13	3.15	4.30
2e	360/22000	475/51	6730	4.2	0.12	0.12	3.04	4.21
2f	381/22000	515/35	6830	6.3	0.06	0.10	2.83	3.90

[a]All values collected in $CHCl_3$. [b]Decay curves fitted using a monoexponential fitting model. [c]Calculated at the PBE0/TZVP level of theory.

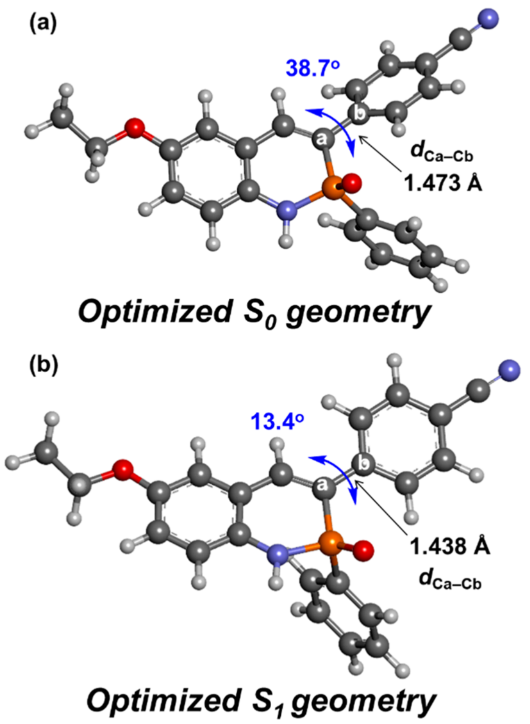

Figure 3. Selected bond length and dihedral angle in the optimized S_0 and S_1 structures of **2f** calculated by DFT and TD-DFT methods at the PCM($CHCl_3$)-PBE0/TZVP level of theory, respectively.

In addition to improved fluorescence properties, we were curious to see how phenyl substitution would affect the strength of hydrogen bond dimerization we typically observe for phosphaquinolinones. Variable concentration (VC) NMR experiments were performed in water-saturated $CDCl_3$ to assess the strength of dimerization (Tables 2 and S17−S21, Figures S14−S23). Heterocycles **2** exhibit dimerization strengths of 22 (for **2e** and **2f**) to 82 M^{-1} (for **2b**). While these values are roughly 70−80% smaller than those measured for the analogous congeners of **1**, the strengths of dimerization for **2** again exceed those of many typical head-to-tail hydrogen bonded dimers.[67] This result suggests that this new entry into the phosphaquinolinone family can still be implemented in supramolecular systems, as found in **1**.[54]

Table 2. Dimerization Constants and Energies for 2

cmpd	K_{dim} (M^{-1})	ΔG_{dim} (kcal mol^{-1})
2a[a]		
2b	82	−2.6
2c	54	−2.3
2d	24	−1.8
2e	22	−1.8
2f	22	−1.8

[a]Not determined because of minimal solubility in H_2O-saturated $CDCl_3$. Values reported with errors less than 15%.

Single crystals suitable for X-ray diffraction were grown by slowly diffusing pentane into a $CHCl_3$ solution of **2f**, and the resultant data are shown in Figures 4 and S1−S3. The

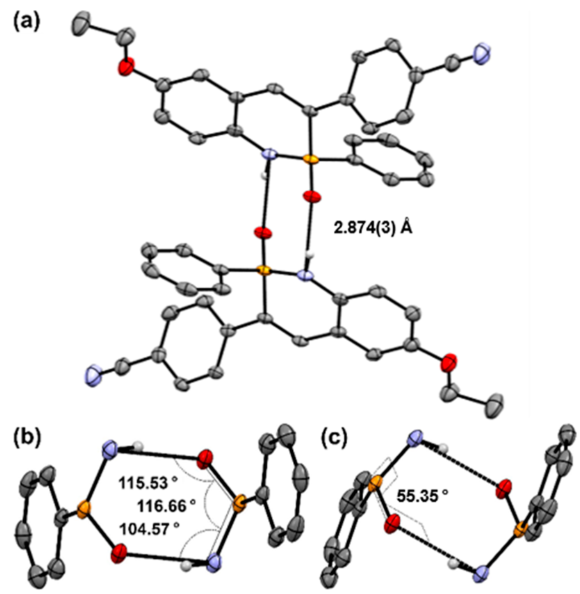

Figure 4. (a) Characteristic PN-heterocycle dimer for **2f** with the O···N distance (Å) shown as well as (b) bond angles and (c) torsional angles formed within monomers upon dimerization. Ellipsoids drawn at 30% probability.

structure of **2f** still features the typical meso-dimer between racemates (Figure 4a); however, the N···O distance in the dimer of **2f** (2.874 Å) is longer than those of heterocycles **1** (2.768−2.821 Å),[40] which supports the observation that the molecule should form a weaker dimer in the solution-state as well. This weakened hydrogen bonding interaction can potentially be explained by examining the pseudo six-membered ring formed between the monomers. The N···O−P (115.53°), O−P−N (116.66°), and P−N···O (104.57°) angles formed between the participating atoms in the dimer formation show significant deviation from the ideal 120° orientation (Figure 4b), likely caused by the large O−P−N−H torsional angle of 55.35° (Figure 4c). With an angle so much larger than the analogous angle found in the crystal structures of several derivatives of **1** (*ca.* 30−40°),[40] there is a less ideal orientation for the two monomers to associate, slightly weakening the interaction overall. By comparing optimized geometries of the *meso*-dimer of **2f** and its −OPh analogue, there are some additional steric clashes in **2f** among the C−H

DOI: 10.1021/acs.joc.9b02132
J. Org. Chem. 2020, 85, 85−91

atoms in the phenyl ring and N−H moieties, according to the noncovalent interactions (NCI) plot (Figure S24). Moreover, the natural bond orbital (NBO) analyses predict a total contribution of the $n_O \rightarrow \sigma_{NH}^*$ interactions of 23.1 kcal mol^{-1} for **2f** and 25.0 kcal mol^{-1} for the respective −OPh analogue (Figure S25). Therefore, the strength of dimerization may decrease to some degree due to the weaker primary hydrogen bonding and extra steric hindrance, in agreement with the observed diminished K_{dim} for **2**.

■ CONCLUSION

In summary, we have shown the effects of the attachment of a phenyl group on the phosphorus center of the phosphaquinolinone scaffold. This new class of PN-heterocycles not only has large Stokes shift values (up to 7000 cm^{-1}) but also shows a marked 4−5-fold increase in the quantum yield when compared to previously reported phenoxy-substituted compounds. Additionally, this modification retains the strong dimerization strengths of the scaffold in both the solid and solution states. This new modification deepens the fundamental understanding of the phosphaquinolinone scaffold and allows for further possibilities in the applications of this scaffold as a biologically or industrially relevant fluorophore, like the coumarin and carbostyril scaffolds.

■ EXPERIMENTAL SECTION

General. All air- or water-free reactions were performed under a N_2 atmosphere using Schlenk techniques. Column chromatography was performed using silica gel (240−300 mesh), with solvent systems being referenced to the most abundant solvent. NMR spectra were acquired at room temperature on a Varian Inova 500 instrument (^{1}H: 500 MHz, ^{13}C: 126 MHz, ^{19}F: 471 MHz, ^{31}P: 202 MHz) or a Bruker Avance III HD 500 apparatus equipped with a Prodigy multinuclear cryoprobe (^{1}H: 500 MHz, ^{13}C: 126 MHz). ^{1}H and ^{13}C chemical shifts (δ) are expressed in parts per million (ppm) relative to residual $CHCl_3$ shifts (^{1}H: 7.26 ppm, ^{13}C: 77.16 ppm) or residual DMSO shifts (^{1}H: 2.50 ppm, ^{13}C: 39.52 ppm). ^{31}P and ^{19}F NMR spectra are referenced to 85% H_3PO_4 (δ 0 ppm) and to $CFCl_3$ (δ 0 ppm), respectively, as the external standards. UV−vis spectra were recorded using an Agilent Technologies Cary 60 UV−vis spectrophotometer in HPLC-grade $CHCl_3$. Fluorescence emission spectra were recorded using a Horiba Jobin Yvon FluoroMax-4 fluorimeter exciting at 365 nm. Quantum yields (ϕ) were determined through a comparison of the emission and absorption intensities of the analyte to that of a 0.1 M H_2SO_4/quinine sulfate solution.[68] Fluorescence lifetime measurements were recorded using a Horiba FluoroHub Single Photon Counting Controller with a TemPro Fluorescence Lifetime System attachment. High-resolution mass spectra (HRMS) were recorded on a Waters XEVO G2-XS mass spectrometer. 2-Ethynylanilines **3a**−**3f**[40] and phenyl diphenylphosphonite ($PhP(OPh)_2$)[69] were prepared as previously described.

General Synthetic Procedure for Phosphaquinolinone 2. 2-Ethynylaniline **3** (1.0 equiv) and $PhP(OPh)_2$ (2.0 equiv) were dissolved in pyridine (ca. 0.35 M). The vessel was sealed and heated to 100 °C for 24 h in an oil bath. The mixture was then diluted with toluene, and the solvent was removed *in vacuo*. This was repeated three times to remove all residual pyridine. The crude material was dissolved in THF, and *ca.* five drops of water were added. The solution was stirred at 60 °C for 1 h before being dried (Na_2SO_4), filtered, and concentrated *in vacuo*. The crude mixture was then purified by column chromatography on silica gel. Reported yields are given for >95% pure material (by ^{1}H NMR spectroscopy), though subsequent recrystallization from hexanes and CH_2Cl_2 was used to achieve analytically pure material.

*Phosphaquinolinone **2a**.* Compound **2a** was synthesized from **3a** (462 mg, 1.9 mmol, 1 equiv) and $PhP(OPh)_2$ (1.11 g, 3.8 mmol, 2 equiv). Column chromatography (1:1 EtOAc:CH_2Cl_2, R_f = 0.20) gave **2a** (149 mg, 21%) as a pale brown solid: mp > 250 °C; ^{1}H NMR (500 MHz, DMSO-d_6) δ 10.28 (d, J = 3.8 Hz, 1H), 8.14 (d, J = 2.0 Hz, 1H), 8.05 (d, J = 30.1 Hz, 1H), 7.82 (*AB*m, J = 8.4 Hz, 4H), 7.81−7.77 (m, 1H), 7.69−7.64 (m, 2H), 7.58−7.51 (m, 1H), 7.49−7.43 (m, 2H), 7.21 (d, J = 8.5 Hz, 1H); ^{13}C{^{1}H} NMR (126 MHz, DMSO-d_6) δ 143.1 (d, J = 3.8 Hz), 140.9 (d, J = 11.7 Hz), 139.3, 135.8, 133.8, 132.6, 132.5 (d, J = 2.7 Hz), 132.4 (d, J = 137.0 Hz), 132.2 (d, J = 10.8 Hz), 128.6 (d, J = 13.2 Hz), 128.1 (d, J = 6.1 Hz), 126.9 (d, J = 115.9 Hz), 119.2, 119.0 (d, J = 9.9 Hz), 118.5, 117.7 (d, J = 8.1 Hz), 110.6, 102.1; ^{31}P{^{1}H} NMR (202 MHz, DMSO-d_6) δ 7.77; HRMS (ASAP) $[M + H]^+$ calcd for $C_{22}H_{15}N_3OP$ 368.0953, found 368.0977.

*Phosphaquinolinone **2b**.* Compound **2b** was synthesized from **3b** (700 mg, 2.4 mmol, 1 equiv) and $PhP(OPh)_2$ (1.40 g, 4.8 mmol, 2 equiv). Recrystallization from CH_2Cl_2 and hexanes gave **2b** (580 mg, 58%) as a yellow solid: mp > 250 °C; ^{1}H NMR (500 MHz, DMSO-d_6) δ 10.14 (d, J = 4.1 Hz, 1H), 8.16 (d, J = 30.1 Hz, 1H), 8.06 (d, J = 2.2 Hz, 1H), 7.85 (d, J = 8.3 Hz, 2H), 7.80 (d, J = 8.4 Hz, 2H), 7.73−7.63 (m, 3H), 7.53 (td, J = 7.4, 1.5 Hz, 1H), 7.49−7.43 (m, 2H), 7.25 (d, J = 8.5 Hz, 1H); ^{13}C{^{1}H} NMR (126 MHz, DMSO-d_6) δ 142.5 (d, J = 3.7 Hz), 141.1 (d, J = 12.0 Hz), 139.9, 132.7 (d, J = 136.9 Hz), 132.6, 132.4 (d, J = 2.7 Hz), 132.2 (d, J = 10.7 Hz), 130.5, 128.5 (d, J = 13.2 Hz), 128.1 (d, J = 6.1 Hz), 127.4 (d, J = 3.7 Hz), 126.5 (d, J = 116.3 Hz), 124.5 (q, J = 271.2 Hz), 120.6 (q, J = 32.3 Hz), 118.6 (d, J = 13.0 Hz), 118.5, 117.4 (d, J = 7.9 Hz), 110.5; ^{31}P{^{1}H} NMR (202 MHz, DMSO-d_6) δ 7.86; ^{19}F NMR (471 MHz, DMSO-d_6) δ −59.92; HRMS (ASAP) $[M + H]^+$ calcd for $C_{22}H_{15}N_2OF_3P$ 411.0874, found 411.0909.

*Phosphaquinolinone **2c**.* Compound **2c** was synthesized from **3c** (645 mg, 2.6 mmol, 1 equiv) and $PhP(OPh)_2$ (1.5 g, 5.1 mmol, 2 equiv). Column chromatography (1:1:1 hexanes:EtOAc:CH_2Cl_2, R_f = 0.10) followed by two rounds of recrystallization from CH_2Cl_2 and hexanes gave **2c** (300 mg, 31%) as a yellow solid: mp > 250 °C; ^{1}H NMR (500 MHz, DMSO-d_6) δ 9.80 (d, J = 4.2 Hz, 1H), 7.99 (d, J = 29.8 Hz, 1H), 7.83 (d, J = 8.4 Hz, 2H), 7.78 (d, J = 8.5 Hz, 2H), 7.73 (d, J = 2.5 Hz, 1H), 7.69−7.57 (m, 2H), 7.56−7.49 (m, 1H), 7.48−7.38 (m, 3H), 7.11 (d, J = 8.7 Hz, 1H); ^{13}C{^{1}H} NMR (126 MHz, DMSO-d_6) δ 141.3 (d, J = 12.0 Hz), 139.4, 138.3 (d, J = 3.7 Hz), 132.8 (d, J = 136.6 Hz), 132.5, 132.3, 132.2, 130.7, 129.9, 128.5 (d, J = 13.1 Hz), 128.1 (d, J = 6.2 Hz), 126.5 (d, J = 116.8 Hz), 123.6, 120.2 (d, J = 12.6 Hz), 118.6, 118.4 (d, J = 8.1 Hz), 110.3; ^{31}P{^{1}H} NMR (202 MHz, DMSO-d_6) δ 7.69; HRMS (ASAP) $[M + H]^+$ calcd for $C_{21}H_{15}N_2OPCl$ 377.0611, found 377.0641.

*Phosphaquinolinone **2d**.* Compound **2d** was synthesized from **3d** (151 mg, 0.69 mmol, 1 equiv) and $PhP(OPh)_2$ (463 mg, 1.4 mmol, 2 equiv). Column chromatography (1:1:1 hexanes:EtOAc:CH_2Cl_2, R_f = 0.20) gave **2d** (144 mg 61%) as a yellow solid: mp > 250 °C; ^{1}H NMR (500 MHz, $CDCl_3$) δ 7.73 (d, J = 8.1 Hz, 2H), 7.66 (d, J = 30.4 Hz, 1H), 7.71−7.66 (m, 2H), 7.54 (d, J = 8.2 Hz, 2H), 7.47−7.42 (m, 2H), 7.38−7.32 (m, 3H), 7.06 (t, J = 7.5 Hz, 1H), 6.97 (d, J = 8.0 Hz, 1H), 6.83 (br s, 1H); ^{13}C{^{1}H} NMR (126 MHz, $CDCl_3$) δ 141.5 (d, J = 11.8 Hz), 141.0 (d, J = 3.0 Hz), 138.8 (d, J = 4.3 Hz), 132.7 (d, J = 10.8 Hz), 132.6 (d, J = 2.8 Hz), 132.5, 132.2 (d, J = 139.3 Hz), 131.5, 131.2, 128.6 (d, J = 13.8 Hz), 128.4 (d, J = 6.2 Hz), 126.0 (d, J = 119.5 Hz), 121.4, 119.4 (d, J = 12.1 Hz), 118.8, 117.3 (d, J = 7.7 Hz), 111.6; ^{31}P{^{1}H} NMR (202 MHz, $CDCl_3$) δ 10.52; HRMS (ASAP) $[M + H]^+$ calcd for $C_{21}H_{16}N_2OP$ 343.1000, found 343.1030.

*Phosphaquinolinone **2e**.* Compound **2e** was synthesized from **3e** (549 mg, 2.0 mmol, 1 equiv) and $PhP(OPh)_2$ (1.3 g, 4.0 mmol, 2 equiv). Column chromatography (1:1:1 EtOAc:CH_2Cl_2, R_f = 0.25) gave **2e** (520 mg, 65%) as a yellow solid: mp > 250 °C; ^{1}H NMR (500 MHz, $CDCl_3$) δ 7.73 (d, J = 8.0 Hz, 2H), 7.72−7.67 (m, 2H), 7.68 (d, J = 30.3 Hz, 1H), 7.53 (d, J = 8.1 Hz, 2H), 7.48−7.39 (m, 3H), 7.37−7.32 (m, 2H), 6.90 (d, J = 8.4 Hz, 1H), 6.48 (br s, 1H), 1.35 (s, 9H); ^{13}C{^{1}H} NMR (126 MHz, $CDCl_3$) δ 144.4, 141.7 (d, J = 12.1 Hz), 141.5, 136.4, 132.7 (d, J = 10.8 Hz), 132.5, 132.5, 132.4 (d, J = 139.2 Hz), 129.1, 128.5 (d, J = 13.6 Hz), 128.4 (d, J = 6.4 Hz), 127.6, 125.8 (d, J = 119.9 Hz), 119.0, 118.9 (d, J = 8.4 Hz), 116.9 (d, J = 7.3 Hz), 111.4, 34.4, 31.5; ^{31}P{^{1}H} NMR (202 MHz, $CDCl_3$) δ

DOI: 10.1021/acs.joc.9b02132
J. Org. Chem. 2020, 85, 85−91

10.44; HRMS (ASAP) $[M + H]^+$ calcd for $C_{25}H_{24}N_2OP$ 399.1628, found 399.1629.

Phosphaquinolinone **2f**. Compound **2f** was synthesized from **3f** (430 mg, 1.7 mmol, 1 equiv) and $PhP(OPh)_2$ (969 g, 3.3 mmol, 2 equiv). Column chromatography (1:1:1 hexanes:EtOAc:CH_2Cl_2, R_f = 0.25) gave **2f** (200 mg, 31%) as a pale yellow solid: mp > 250 °C; ^1H NMR (500 MHz, $CDCl_3$) δ 7.73−7.65 (m, 2H), 7.71 (d, J = 8.6 Hz, 2H), 7.59 (d, J = 30.4 Hz, 1H), 7.53 (d, J = 8.2 Hz, 2H), 7.47−7.42 (m, 1H), 7.37−7.31 (m, 2H), 6.98−6.93 (m, 2H), 6.88 (d, J = 8.5 Hz, 1H), 6.60 (br s, 1H), 4.04 (q, J = 7.0 Hz, 2H), 1.43 (t, J = 7.0 Hz, 3H); $^{13}C\{^1H\}$ NMR (126 MHz, $CDCl_3$) δ 153.5, 141.6 (d, J = 12.0 Hz), 140.7, 132.8 (d, J = 10.7 Hz), 132.7, 132.6 (d, J = 3.0 Hz), 132.5, 132.1 (d, J = 140.4 Hz), 128.5 (d, J = 13.8 Hz), 128.4 (d, J = 6.4 Hz), 126.7 (d, J = 119.9 Hz), 119.9, 119.8 (d, J = 11.8 Hz), 118.8, 118.2 (d, J = 7.7 Hz), 114.8, 111.5, 64.3, 15.0; $^{31}P\{^1H\}$ NMR (202 MHz, $CDCl_3$) δ 10.51; HRMS (ASAP) $[M + H]^+$ calcd for $C_{23}H_{20}N_2O_2P$ 387.1261, found 387.1283.

■ ASSOCIATED CONTENT

Supporting Information

The Supporting Information is available free of charge on the ACS Publications website at DOI: 10.1021/acs.joc.9b02132.

NMR spectra for all new compounds, X-ray structure data and molecular packing, computational details (including the coordinates of optimized structures), and self-dimerization study data (PDF)

Crystallographic information for **2f** (CCDC No. 1944053) (CIF)

■ AUTHOR INFORMATION

Corresponding Authors

*E-mail: dwj@uoregon.edu.

*E-mail: haley@uoregon.edu.

ORCID

Jeremy P. Bard: 0000-0001-6135-0977

Hannah J. Bates: 0000-0003-2019-2196

Chun-Lin Deng: 0000-0002-3192-9424

Darren W. Johnson: 0000-0001-5967-5115

Michael M. Haley: 0000-0002-7027-4141

Notes

The authors declare no competing financial interest.

■ ACKNOWLEDGMENTS

We thank the National Science Foundation (INFEWS CHE-1607214) for support of this research. We are grateful to Joshua E. Barker for obtaining the HRMS via a CAMCOR facility supported by the NSF (CHE-1625529). This work was also supported by the Bradshaw and Holzapfel Research Professorship in Transformational Science and Mathematics to D.W.J.

■ REFERENCES

(1) Lavis, L. D.; Raines, R. T. Bright Ideas for Chemical Biology. *ACS Chem. Biol.* **2008**, *3*, 142−155.

(2) Basabe-Desmonts, L.; Reinhoudt, D. N.; Crego-Calama, M. Design of Fluorescent Materials for Chemical Sensing. *Chem. Soc. Rev.* **2007**, *36*, 993−1017.

(3) Vendrell, M.; Zhai, D.; Er, J. C.; Chang, Y.-T. Combinatorial Strategies in Fluorescent Probe Development. *Chem. Rev.* **2012**, *112*, 4391−4420.

(4) Du, J.; Hu, M.; Fan, J.; Peng, X. Fluorescent Chemodosimeters Using "Mild" Chemical Events for the Detection of Small Anions and Cations in Biological and Environmental Media. *Chem. Soc. Rev.* **2012**, *41*, 4511−4535.

(5) Tabaković, I.; Tabaković, K.; Trkovnik, M.; Stunic, Z. Chemistryof Coumarins. Annelationof CoumarinRing*via* Reactionsof 3-Amino-4-hydroxycoumarin. *Org. Prep. Proced. Int.* **1985**, *17*, 133−137.

(6) Song, Y.; Chen, Z.; Li, H. Advances in Coumarin-Derived Fluorescent Chemosensors for Metal Ions. *Curr. Org. Chem.* **2012**, *16*, 2690−2707.

(7) Stefanachi, A.; Leonetti, F.; Pisani, L.; Catto, M.; Carotti, A. Coumarin: A Natural, Privileged and Versatile Scaffold for Bioactive Compounds. *Molecules* **2018**, *23*, 250−284.

(8) Becker, R. S.; Chakravorti, S.; Gartner, C. A.; de Graca Miguel, M. Photosensitizers: Comprehensive Photophysics/Photochemistry and Theory of Coumarins, Chromones, Their Homologues and Thione Analogues. *J. Chem. Soc., Faraday Trans.* **1993**, *89*, 1007−1019.

(9) Sethna, S. M.; Shah, N. M. The Chemistry of Coumarins. *Chem. Rev.* **1945**, *36*, 1−62.

(10) Tabaković, K.; Tabaković, I. Chemistry of Coumarins. Thermal Reactions of 4-Chloro-3-coumarinyl *N,N*-Dialkyldithiocarbamates and 3-Nitro-4-coumarinyl *N*-Phenyldithiocarbamate. *J. Heterocycl. Chem.* **1992**, *29*, 383−385.

(11) Pereira, T. M.; Franco, D. P.; Vitorio, F.; Kummerle, A. E. Coumarin Compounds in Medicinal Chemistry: Some Important Examples from the Last Years. *Curr. Top. Med. Chem.* **2018**, *18*, 124−148.

(12) Riveiro, M. E.; De Kimpe, N.; Moglioni, A.; Vázquez, R.; Monczor, F.; Shayo, C.; Davio, C. Coumarins: Old Compounds with Novel Promising Therapeutic Perspectives. *Curr. Med. Chem.* **2010**, *17*, 1325−1338.

(13) Cao, D.; Liu, Z.; Verwilst, P.; Koo, S.; Jangjili, P.; Kim, J. S.; Lin, W. Coumarin-Based Small-Molecule Fluorescent Chemosensors. *Chem. Rev.* **2019**, *119*, 10403−10519.

(14) Abernethy, J. L. The Historical and Current Interest in Coumarin. *J. Chem. Educ.* **1969**, *46*, 561−568.

(15) Harborne, J. B. The Natural Coumarins: Occurrence, Chemistryand Biochemistry. *Plant, Cell Environ.* **1982**, *5*, 435−436.

(16) Anamika; Utreja, D.; Ekta; Jain, N.; Sharma, S. Advances in Synthesis and Potentially Bioactive of Coumarin Derivatives. *Curr. Org. Chem.* **2019**, *22*, 2509−2536.

(17) Govori, S. Convenient Methods for the Synthesis of Pentacyclic Fused Heterocycles with Coumarin Moiety. *Synth. Commun.* **2016**, *46*, 569−580.

(18) Medina, F. G.; Marrero, J. G.; Macías-Alonso, M.; González, M. C.; Córdova-Guerrero, I.; Teissier García, A. G.; Osegueda-Robles, S. Coumarin Heterocyclic Derivatives: Chemical Synthesis and Biological Activity. *Nat. Prod. Rep.* **2015**, *32*, 1472−1507.

(19) Tasior, M.; Kim, D.; Singha, S.; Krzeszewski, M.; Ahn, K. H.; Gryko, D. T. *π*-Expanded Coumarins: Synthesis, Optical Properties and Applications. *J. Mater. Chem. C* **2015**, *3*, 1421−1446.

(20) Liu, X.; Xu, Z.; Cole, J. M. Molecular Design of UV−Vis Absorption and Emission Properties in Organic Fluorophores: Toward Larger Bathochromic Shifts, Enhanced Molar Extinction Coefficients, and Greater Stokes Shifts. *J. Phys. Chem. C* **2013**, *117*, 16584−16595.

(21) Nad, S.; Kumbhakar, M.; Pal, H. Photophysical Properties of Coumarin-152 and Coumarin-481 Dyes: Unusual Behavior in Nonpolar and in Higher Polarity Solvents. *J. Phys. Chem. A* **2003**, *107*, 4808−4816.

(22) Jones, G.; Rahman, M. A. Fluorescence Properties of Coumarin Laser Dyes in Aqueous Polymer Media. Chromophore Isolation in Poly(methacrylic acid) Hypercoils. *J. Phys. Chem.* **1994**, *98*, 13028−13037.

(23) Cisse, L.; Djande, A.; Capo-Chichi, M.; Delatre, F.; Saba, A.; Tine, A.; Aaron, J.-J. Revisiting the Photophysical Properties and Excited Singlet-State Dipole Moments of Several Coumarin Derivatives. *Spectrochim. Acta, Part A* **2011**, *79*, 428−436.

(24) Cigán, M.; Donovalová, J.; Szöcs, V.; Gašpar, J.; Jakusová, K.; Gáplovský, A. 7-(Dimethylamino)coumarin-3-carbaldehyde and Its Phenylsemicarbazone: TICT Excited State Modulation, Fluorescent

H-Aggregates, and Preferential Solvation. *J. Phys. Chem. A* **2013**, *117*, 4870−4883.
(25) Gandioso, A.; Bresolí-Obach, R.; Nin-Hill, A.; Bosch, M.; Palau, M.; Galindo, A.; Contreras, S.; Rovira, A.; Rovira, C.; Nonell, S.; Marchán, V. Redesigning the Coumarin Scaffold into Small Bright Fluorophores with Far-Red to Near-Infrared Emission and Large Stokes Shifts Useful for Cell Imaging. *J. Org. Chem.* **2018**, *83*, 1185−1195.
(26) Wang, Z.-S.; Cui, Y.; Hara, K.; Dan-Oh, Y.; Kasada, C.; Shinpo, A. A High-Light-Harvesting-Efficiency Coumarin Dye for Stable Dye-Sensitized Solar Cells. *Adv. Mater.* **2007**, *19*, 1138−1141.
(27) Bu, F.; Duan, R.; Xie, Y.; Yi, Y.; Peng, Q.; Hu, R.; Qin, A.; Zhao, Z.; Tang, B. Z. Unusual Aggregation-Induced Emission of a Coumarin Derivative as a Result of the Restriction of an Intramolecular Twisting Motion. *Angew. Chem., Int. Ed.* **2015**, *54*, 14492−14497.
(28) Chen, J.-X.; Liu, W.; Zheng, C.-J.; Wang, K.; Liang, K.; Shi, Y.-Z.; Ou, X.-M.; Zhang, X.-H. Coumarin-Based Thermally Activated Delayed Fluorescence Emitters with High External Quantum Efficiency and Low Efficiency Roll-off in the Devices. *ACS Appl. Mater. Interfaces* **2017**, *9*, 8848−8854.
(29) Hara, K.; Sato, T.; Katoh, R.; Furube, A.; Ohga, Y.; Shinpo, A.; Suga, S.; Sayama, K.; Sugihara, H.; Arakawa, H. Molecular Design of Coumarin Dyes for Efficient Dye-Sensitized Solar Cells. *J. Phys. Chem. B* **2003**, *107*, 597−606.
(30) Swanson, S. A.; Wallraff, G. M.; Chen, J. P.; Zhang, W.; Bozano, L. D.; Carter, K. R.; Salem, J. R.; Villa, R.; Scott, J. C. Stable and Efficient Fluorescent Red and Green Dyes for External and Internal Conversion of Blue OLED Emission. *Chem. Mater.* **2003**, *15*, 2305−2312.
(31) Jung, Y.; Jung, J.; Huh, Y.; Kim, D. Benzo[*g*]Coumarin-Based Fluorescent Probes for Bioimaging Applications. *J. Anal. Methods Chem.* **2018**, *2018*, 1−11.
(32) Ahvale, A. B.; Prokopcová, H.; Šefčovičová, J.; Steinschifter, W.; Täubl, A. E.; Uray, G.; Stadlbauer, W. 4-Cyano-6,7-dimethoxycarbostyrils with Solvent- and PH-Independent High Fluorescence Quantum Yields and Emission Maxima. *Eur. J. Org. Chem.* **2008**, *2008*, 563−571.
(33) de Macedo, M. B.; Kimmel, R.; Urankar, D.; Gazvoda, M.; Peixoto, A.; Cools, F.; Torfs, E.; Verschaeve, L.; Lima, E. S.; Lyčka, A.; Milićević, D.; Klásek, A.; Cos, P.; Kafka, S.; Košmrlj, J.; Cappoen, D. Design, Synthesis and Antitubercular Potency of 4-Hydroxyquinolin-2(1H)-ones. *Eur. J. Med. Chem.* **2017**, *138*, 491−500.
(34) Enoua, G. C.; Lahm, G.; Uray, G.; Stadlbauer, W. Syntheses and Fluorescent Properties of 6-Methoxy-2-oxoquinoline-3,4-dicarbonitriles and 6,7-Dimethoxy-2-oxoquinoline-3,4-dicarbonitriles. *J. Heterocycl. Chem.* **2014**, *51*, E263−E275.
(35) Strohmeier, G. A.; Fabian, W. M. F.; Uray, G. A Combined Experimental and Theoretical Approach Toward the Development of Optimized Luminescent Carbostyrils. *Helv. Chim. Acta* **2004**, *87*, 215−226.
(36) Uray, G.; Niederreiter, K. S.; Belaj, F.; Fabian, W. M. F. Long-Wavelength-Absorbing and -Emitting Carbostyrils with High Fluorescence Quantum Yields. *Helv. Chim. Acta* **1999**, *82*, 1408−1417.
(37) Fabian, W. M. F.; Niederreiter, K. S.; Uray, G.; Stadlbauer, W. Substituent Effects on Absorption and Fluorescence Spectra of Carbostyrils. *J. Mol. Struct.* **1999**, *477*, 209−220.
(38) Tashima, T. The Structural Use of Carbostyril in Physiologically Active Substances. *Bioorg. Med. Chem. Lett.* **2015**, *25*, 3415−3419.
(39) Casley-Smith, J. R.; Morgan, R. G.; Piller, N. B. Treatment of Lymphedema of the Arms and Legs with 5,6-Benzo-[α]-pyrone. *N. Engl. J. Med.* **1993**, *329*, 1158−1163.
(40) Bard, J. P.; Deng, C.-L.; Richardson, H. C.; Odulio, J. M.; Barker, J. E.; Zakharov, L. N.; Cheong, P. H.-Y.; Johnson, D. W.; Haley, M. M. Synthesis, Photophysical Properties, and Self-Dimerization Studies of 2-λ^5-Phosphaquinolin-2-ones. *Org. Chem. Front.* **2019**, *6*, 1257−1265.
(41) Vonnegut, C. L.; Shonkwiler, A. M.; Khalifa, M. M.; Zakharov, L. N.; Johnson, D. W.; Haley, M. M. Facile Synthesis and Properties of 2-λ^5-Phosphaquinolines and 2-λ^5-Phosphaquinolin-2-ones. *Angew. Chem., Int. Ed.* **2015**, *54*, 13318−13322.
(42) Dewar, M. J. S.; Kubba, V. P. New Heteroaromatic Compounds. Part VI. Novel Heterocyclic Compounds of Phosphorus. *J. Am. Chem. Soc.* **1960**, *82*, 5685−5688.
(43) Campbell, I. G. M.; Way, J. K. Synthesis and Stereochemistry of Heterocyclic Phosphorus Compounds. Part I. Preparation of (+)- and (−)-10-p-Dimethylaminophenyl-9,10-Dihydro-9-Aza-10-Phosphaphenanthrene. *J. Chem. Soc.* **1960**, *0*, 5034−5041.
(44) Sun, Y.; Cramer, N. Rhodium(III)-Catalyzed Enantiotopic C-H Activation Enables Access to *P* -Chiral Cyclic Phosphinamides. *Angew. Chem., Int. Ed.* **2017**, *56*, 364−367.
(45) Tang, W.; Ding, Y. X. Synthesis of Phosphaisoquinolin-1-Ones by Pd(II)-Catalyzed Cyclization of *o*-(1-Alkynyl)-Phenylphosphonamide Monoesters. *J. Org. Chem.* **2006**, *71*, 8489−8492.
(46) Yan, J. H.; Li, Q. Y.; Boutin, J. A.; Renard, M. P.; Ding, Y. X.; Hao, X. J.; Zhao, W. M.; Wang, M. W. High-Throughput Screening of Novel Antagonists on Melanin-Concentrating Hormone Receptor-1. *Acta Pharmacol. Sin.* **2008**, *29*, 752−758.
(47) Zhao, D.; Nimphius, C.; Lindale, M.; Glorius, F. Phosphoryl-Related Directing Groups in Rhodium(III) Catalysis: A General Strategy to Diverse P-Containing Frameworks. *Org. Lett.* **2013**, *15*, 4504−4507.
(48) Park, S.; Seo, B.; Shin, S.; Son, J.-Y.; Lee, P. H. Rhodium-Catalyzed Oxidative Coupling through C−H Activation and Annulation Directed by Phosphonamide and Phosphinamide Groups. *Chem. Commun.* **2013**, *49*, 8671−8673.
(49) Liu, L.; Zhang, A.-A.; Wang, Y.; Zhang, F.; Zuo, Z.; Zhao, W.-X.; Feng, C.-L.; Ma, W. Asymmetric Synthesis of P-Stereogenic Phosphinic Amides via Pd(0)-Catalyzed Enantioselective Intramolecular C−H Arylation. *Org. Lett.* **2015**, *17*, 2046−2049.
(50) Lin, Z.-Q.; Wang, W.-Z.; Yan, S.-B.; Duan, W.-L. Palladium-Catalyzed Enantioselective C−H Arylation for the Synthesis of P-Stereogenic Compounds. *Angew. Chem., Int. Ed.* **2015**, *54*, 6265−6269.
(51) Wang, Z.; Gelfand, B. S.; Baumgartner, T. Hydrogen Bonding Dithienophosphole-Based Phosphinamides with Intriguing Self-Assembly Behavior. *Angew. Chem., Int. Ed.* **2016**, *55*, 3481−3485.
(52) Ma, Y.-N.; Zhang, X.; Yang, S. Tandem Oxidative C-H Amination and Iodization to Synthesize Difunctional Atropoisomeric P-Stereogenic Phosphinamides. *Chem. - Eur. J.* **2017**, *23*, 3007−3011.
(53) Takaesu, N. A.; Ohta, E.; Zakharov, L. N.; Johnson, D. W.; Haley, M. M. Synthesis and Properties of Naphtho[2,3-*e*]-1,2-azaphosphorine-2-oxides: PN-Anthracene Analogues. *Organometallics* **2017**, *36*, 2491−2493.
(54) Deng, C.-L.; Bard, J. P.; Lohrman, J. A.; Barker, J. E.; Zakharov, L. N.; Johnson, D. W.; Haley, M. M. Exploiting the Hydrogen Bond Donor/Acceptor Properties of PN-Heterocycles: Selective Anion Receptors for Hydrogen Sulfate. *Angew. Chem., Int. Ed.* **2019**, *58*, 3934−3938.
(55) Deng, C.-L.; Bard, J. P.; Zakharov, L. N.; Johnson, D. W.; Haley, M. M. Naphtho[2,1-*e*]-1,2-azaphosphorine 2-oxide Derivatives: Synthesis, Optoelectronic Properties, and Self-Dimerization Phenomena. *J. Org. Chem.* **2019**, *84*, 8131−8139.
(56) Deng, C.-L.; Bard, J. P.; Zakharov, L. N.; Johnson, D. W.; Haley, M. M. PN-Containing Pyrene Derivatives: Synthesis, Structure, and Photophysical Properties. *Org. Lett.* **2019**, *21*, 6427−6431.
(57) Schaub, T. A.; Brülls, S. M.; Dral, P. O.; Hampel, F.; Maid, H.; Kivala, M. Organic Electron Acceptors Comprising a Dicyanomethylene-Bridged Acridophosphine Scaffold: The Impact of the Heteroatom. *Chem. - Eur. J.* **2017**, *23*, 6988−6992.
(58) Romero-Nieto, C.; Lõpez-Andarias, A.; Egler-Lucas, C.; Gebert, F.; Neus, J. P.; Pilgram, O. Paving the Way to Novel Phosphorus-Based Architectures: A Noncatalyzed Protocol to Access Six-Membered Heterocycles. *Angew. Chem., Int. Ed.* **2015**, *54*, 15872−15875.

DOI: 10.1021/acs.joc.9b02132
J. Org. Chem. 2020, 85, 85−91

(59) Fukazawa, A.; Osaki, H.; Yamaguchi, S. Hydroxyphenyl-Substituted Benzophosphole Oxides: Impact of the Intramolecular Hydrogen Bond on the Fluorescence Properties. *Asian J. Org. Chem.* **2014**, *3*, 122−127.
(60) Regulska, E.; Romero-Nieto, C. Highlights on π-Systems Based on Six-Membered Phosphorus Heterocycles. *Dalt. Trans.* **2018**, *47*, 10344−10359.
(61) Grenon, N.; Baumgartner, T. Exploration of Hypervalent Lewis Acid/Base Interactions in 2-(2'-Thiazolyl)-3-Thienylphosphanes. *Inorg. Chem.* **2018**, *57*, 1630−1644.
(62) Gong, P.; Ye, K.; Sun, J.; Chen, P.; Xue, P.; Yang, H.; Lu, R. Electroluminescence and Fluorescence Response towards Acid Vapors Depending on the Structures of Indole-Fused Phospholes. *RSC Adv.* **2015**, *5*, 94990−94996.
(63) Jiang, X. D.; Zhao, J.; Xi, D.; Yu, H.; Guan, J.; Li, S.; Sun, C. L.; Xiao, L. J. A New Water-Soluble Phosphorus-Dipyrromethene and Phosphorus-Azadipyrromethene Dye: PODIPY/Aza-PODIPY. *Chem. - Eur. J.* **2015**, *21*, 6079−6082.
(64) Mathey, F. The Organic Chemistry of Phospholes. *Chem. Rev.* **1988**, *88*, 429−453.
(65) Avarvari, N.; Le Floch, P.; Mathey, F. 1,3,2-Diazaphosphinines: New Versatile Precursors of 1,2-Azaphosphinines and Polyfunctional Phosphinines. *J. Am. Chem. Soc.* **1996**, *118*, 11978−11979.
(66) Sun, W.-C.; Gee, K. R.; Haugland, R. P. Synthesis of Novel Fluorinated Coumarins: Excellent UV-Light Excitable Fluorescent Dyes. *Bioorg. Med. Chem. Lett.* **1998**, *8*, 3107−3110.
(67) See the detailed list of similar dimers in the SI of: Quinn, J. R.; Zimmerman, S. C.; Del Bene, J. E.; Shavitt, I. Does the A.T or G.C Base-Pair Possess Enhanced Stability? Quantifying the Effects of CH···O Interactions and Secondary Interactions on Base-Pair Stability Using a Phenomenological Analysis and ab initio Calculations. *J. Am. Chem. Soc.* **2007**, *129*, 934−941.
(68) Brouwer, A. M. Standards for Photoluminescence Quantum Yield Measurements in Solution. *Pure Appl. Chem.* **2011**, *83*, 2213−2228.
(69) Kuroda, K.; Maruyama, Y.; Hayashi, Y.; Mukaiyama, T. Conversion of Alcohols to Alkyl Aryl Sulfides by a New Type of Oxidation−Reduction Condensation Using Phenyl Diphenylphosphinite. *Bull. Chem. Soc. Jpn.* **2009**, *82*, 381−392.

DOI: 10.1021/acs.joc.9b02132
J. Org. Chem. 2020, 85, 85−91